Nonfission Inelastic Events in Uranium and Thorium Induced by High-Energy Protons*

M. LINDNER AND R. N. OSBORNE
University of California Radiation Laboratory, Livermore, California
(Received March 20, 1956)

Activation cross sections for about thirty products of high-energy proton-induced disintegration of U^{238} and Th^{232} have been measured by the radiochemical method. These products range from polonium ($Z=84$) to neptunium ($Z=93$). The energy dependence of some of these cross sections has been determined for formation from U^{238}. Because of fission competition, the spallation cross section of U^{238} is considerably less than that of Th^{232}. The data suggest that light isotopes of uranium are primarily responsible for the fission generally associated with high-energy particle bombardment of U^{238}.

INTRODUCTION

SINCE the advent of accelerators producing particles of energies in the hundred-million-electron-volt region, rather extensive radiochemical studies have been made of the disintegration products of a large number of elements. These studies include proton interactions with copper,[1] cobalt,[2,3] iron,[4] silver,[5] cesium,[6] tantalum,[7] and bismuth,[8] deuteron interactions with arsenic[9] and antimony,[10] and helium-ion spallation of uranium.[11] In general the interpretations of these studies have met with varying degrees of success, due in part to the limitations imposed by counting techniques, and in part to the complexity of the interactions. The use of polyisotopic elements and of bombarding particles containing more than one nucleon further complicate the interpretation of results. For these reasons it has not been possible to formulate a wholly consistent and unified interpretation of the radiochemical data available for such inelastic interactions. It can nevertheless be said that, in their most general features, all radiochemical results are at least consistent with Serber's model[12] for high-energy nuclear reactions, in which the incoming particles with wavelengths short in comparison with, but mean free paths of the order of, nuclear dimensions, interact with nuclei through collisions with individual nucleons. Nuclear evaporation theory[13] could then be used to predict the effects of residual nuclear excitation.

The study of the spallation products of U^{238} and Th^{232} by the radiochemical method seemed to offer certain unique advantages over similar studies with other elements:

(1) Effectively only one isotope need be considered in interpretation of the results.

(2) Because many of the resultant nuclei are unstable toward alpha-particle emission, a number of beta-stable products can be measured which would otherwise escape detection by activation techniques.

(3) Many of the neutron-deficient nuclides produced in the irradiation of U^{238} and Th^{232} decay primarily through alpha-particle emission rather than through the orbital capture process. The absolute measurement of decay rates is much easier for alpha emitters than for nuclides decaying by ortibal capture.

It is also true, however, the occurrence of alpha-particle decay in this region poses certain unique difficulties not encountered elsewhere in such investigations; many radioactive products have as their origin not only the initial inelastic event but they may also arise as daughter nuclei of either alpha- or beta-unstable products; sometimes both decay modes contribute to an observed product.

O'Connor and Seaborg[11] measured the yields of several spallation products of uranium in bombardments with 380-Mev helium ions.

From recent measurements on inelastic and fission cross sections of U^{238} it has become possible to estimate the nonfission inelastic cross section in uranium irradiated with high-energy protons; Crandall *et al.*[14] have listed the total inelastic scattering cross section of uranium as roughly 1.7–1.8 barns for 300-Mev protons. On the other hand, the fission cross section of U^{238} for 340-Mev protons has been established by fission counting[15] and by radiochemical investigation[16] to be about 1.5 barns. A difference of 0.2–0.3 barn may thus be ascribed to the spallation portion of the inelastic cross section. In the present radiochemical investigation, this cross section has been obtained by integration of the cross sections for all observed and interpolated spallation products arising from bombardment of U^{238}

* Work performed under former contract AT(11-1)-74 of the California Research and Development Company with the U. S. Atomic Energy Commission.

[1] Batzel, Miller, and Seaborg, Phys. Rev. **84**, 671 (1951).
[2] E. Belmont and J. M. Miller, Phys. Rev. **95**, 1554 (1954).
[3] G. D. Wagner and E. O. Wiig, Phys. Rev. **96**, 1100 (1954).
[4] Rudstam, Stevenson, and Folger, Phys. Rev. **87**, 358 (1952).
[5] P. K. Kofstad, University of California Radiation Laboratory Report UCRL-2265 (unpublished).
[6] R. W. Fink and E. O. Wiig, Phys. Rev. **94**, 1357 (1954).
[7] W. E. Nervik and G. T. Seaborg, Phys. Rev. **97**, 1092 (1955).
[8] W. E. Bennett, Phys. Rev. **94**, 997 (1954).
[9] H. H. Hopkins, University of California Radiation Laboratory Report UCRL-312 (unpublished).
[10] M. Lindner and I. Perlman, Phys. Rev. **78**, 499 (1950).
[11] P. R. O'Connor and G. T. Seaborg, Phys. Rev. **74**, 1189 (1948).
[12] R. Serber, Phys. Rev. **72**, 1114 (1947).
[13] V. F. Weisskopf, Phys. Rev. **52**, 295 (1937).
[14] Millburn, Birnbaum, Crandall, and Schechter, Phys. Rev. **95**, 1268 (1954).
[15] J. Jungerman and H. M. Steiner, Phys. Rev. **101**, 807 (1956).
[16] H. G. Hicks and R. S. Gilbert, Phys. Rev. **100**, 1286 (1955).

TABLE I. Spallation product yields (in millibarns) of uranium irradiated with high-energy protons.

Nuclide \ Energy (Mev)	100	125	140	150	160	175	190	200	220	250	270	300	340
Np238	...	...	...	...	...	...	...	...	...	...	...	...	0.46±0.05
236	...	...	...	...	...	...	...	...	...	...	...	...	1.7±0.1
U237[a]	93	...	...	73	...	...	...	67.5	...	...	...	81	85
232	...	...	...	...	...	...	...	...	...	...	...	...	≤4
230	0.41±.03	...	0.63±0.03	0.67	0.49±0.01	0.57	...	0.41	0.43	0.40	...	0.34	0.35±0.12
229	0.046	0.064	0.093±0.01	0.11	0.08±0.01	0.092	...	0.10	0.076	0.069	...	0.056	0.060±0.005
228	0.012	0.031	0.047±0.01	0.046	0.036±0.001	0.038	...	0.030	0.035	0.037	...	0.032	0.038±0.002
Pa235	5.7±0.5	...	...	...	...	7.3±0.5	...	...	...	15.1±0.2	...	...	21±2
232	...	...	...	...	...	...	...	...	...	...	...	...	8.7±1
230	1.5±0.2	...	...	3.7	...	...	3.6	...	...	...	4.8±0.4	...	5.1±0.5
228	...	...	...	...	...	...	...	...	...	...	...	...	1.7±0.2
227[b]	0.086	0.20	...	0.30	...	0.46	0.56	0.62	0.68	0.71	0.71	0.71	0.71±0.06
Th234	0.95±0.1	...	...	1.8	...	...	1.1	...	...	...	...	2.5	1.8±0.7
231	0.50±0.05	...	...	1.0	...	...	1.1	...	...	...	1.7	...	2.4±0.1
228	0.85	...	...	0.9	...	...	0.95	...	...	...	1.9	...	2.9±0.9
227	0.32±0.01	...	...	0.9	...	...	1.3	...	...	...	2.3±0.2	...	3.3±0.4
226	...	...	...	...	...	...	...	...	...	...	...	...	2.7±0.2
Ac228	...	...	...	...	...	...	...	...	...	...	...	...	0.62±0.08
226	0.021	...	...	0.07	...	...	0.24	...	...	...	0.38	...	0.54±0.09
225	0.011	...	...	0.009	...	...	0.26	...	...	...	0.41	...	0.62±0.13
224	...	...	...	...	...	...	...	...	...	...	...	...	1.05±0.05
Ra228	...	...	...	...	...	...	...	...	...	...	...	...	0.043
225	...	...	...	...	...	...	...	...	...	...	...	...	0.26±0.02
224	0.017	...	...	0.09	...	...	...	0.26	...	...	0.44	...	0.58±0.18
223	...	...	...	...	...	...	...	...	...	...	...	...	0.48±0.11

[a] Includes yield of Pa^{237}; unpublished data from Tellefsen (see reference 18).
[b] Excitation function from Meinke (see reference 19).

and Th^{232} with 340-Mev protons. In addition, an attempt has been made to compare the extent of fission-spallation competition for these two nuclides; it is known, for example from direct fission cross-section measurements,[15] that the fission cross section of Th^{232} is only about 0.8 barn, as compared to 1.5 barns for U^{238}. Since the total inelastic cross sections for these nuclides should be very nearly equal, it is of interest to determine whether the remainder of this cross section can be accounted for in spallation-type events in Th^{232}.

EXPERIMENTAL PROCEDURE

Irradiations

Uranium and thorium foils from one to ten mils in thickness were bombarded for periods varying from several mintes to several hours in the Berkeley 184-inch cyclotron with protons in the internal circulating beam. The proton energies ranged from 100 Mev to 340 Mev.

Beam intensities were determined by comparison with the Na^{24} induced in an aluminum monitor foil intercepting the same flux as the uranium or thorium foil. The cross section for formation of a given spallation product was thus based upon the value for the known cross section for Na^{24} formation in aluminum by protons of a given energy.[17]

Chemical Procedures

Isotopes of neptunium, uranium, protactinium, thorium, actinium, radium, and polonium from uranium targets, and isotopes of protactinium, thorium, actinium, radium, and polonium from thorium targets, were studied.

The occurrence of alpha-particle emission among the nuclides in this region makes possible—and, in many cases, necessary—the use of chemical separation techniques not employed with elements of lower atomic number for which carriers are usually available. Therefore, chemical yields were generally determined through the use of tracer quantities of a long-lived radioactive species isotopic with the nuclide of interest.

The separations technique in general consisted in dissolving the uranium or thorium target in an appropriate medium and, following the addition of the proper tracers, in isolating the respective elemental fractions.

A brief account is given in Appendix A of the chemical separation procedures, and of the methods of radiation detection; no attempt has been made to provide exhaustive details of the isolation and final purification.

Experimental Results

Table I gives the mean cross sections for all measured spallation products of uranium at a series of energies from 100 to 340 Mev. In Table II are given the mean cross sections for formation of spallation products of thorium induced with 340-Mev protons.

The measurable cross section for the sum of the U^{237} and Pa^{237} formation was obtained from Tellefsen[18] and is included here because of the importance of this cross section to the present work. The data for the energy-dependence of the Pa^{227} formation cross section were taken from an excitation function of Meinke[19] and fitted to the observed average value at 340 Mev.

The limits of accuracy shown in Tables I and II represent the mean deviation for those cases for which multiple determinations had been made. Sources of inaccuracy are inherent in the radiochemical method which would be extremely difficult to assess, and which must be inferred in all values reported in Tables I and

[17] Hicks, Stevenson, and Nervik, Phys. Rev. **102**, 1390 (1956).

[18] R. L. Tellefesen (private communication).

[19] W. W. Meinke (unpublished data).

TABLE II. Mean cross sections for formation of spallation products of thorium irradiated with 340-Mev protons.

Nuclide	σ(mb)
Pa232	2.6±1.2
230	4.2±0.3
228	1.7±0.2
227	1.0±0.2
Th231[a]	68±3
228	30±3
227	22±5
226	17±0.3
Ac228	28±0.1
227	14±0.8
226	10±1.6
225	14±3
224	12.5±0.9
Ra227	>0.7
225	2.1±0.5
224	8.0±1.5
223	6.7±1.4

[a] Includes independent yield of Ac^{231}.

II. Included would be errors resulting from imperfections in alignment of target and monitor foils, absorption of alpha rays by finite sample thickness, and the over-all accumulation of calculable counting errors in decay and in alpha-particle pulse-height analysis. In some instances the determination of cross sections depended not only upon the factors mentioned but also upon parent-daughter separations with additional tracer measurements and pulse analyses. Thus the accumulated errors would sometimes become rather large. An extreme example is the determination of the Pa^{232} formation cross section from bombardment of thorium. This value was obtained by allowing the Pa^{232} to decay to the U^{232} daughter, then chemically separating the daughter along with added U^{234} tracer. The level of the pulse-analyzed U^{232} activity was exceedingly low, so that large errors were not unexpected. Consequently agreement of four separate determinations to within a factor of four was the best that could be obtained. In still other cases the independent yields were obtained only after correction for formation from decay of one or more radioactive parent nuclides. An example is Th^{228}, which can arise independently as a daughter activity from the decay of either Ac^{228}, Pa^{228}, or U^{232}.

Figures 1 and 2 represent the data obtained at 340 Mev for U^{238} and Th^{232}, respectively. The experimental values from each bombardment have been plotted, rather than the mean values (with mean deviation) given in Tables I and II.

The independent yields for U^{237} and Pa^{237} and for Th^{231} and Ac^{231} were calculated on the assumption that,

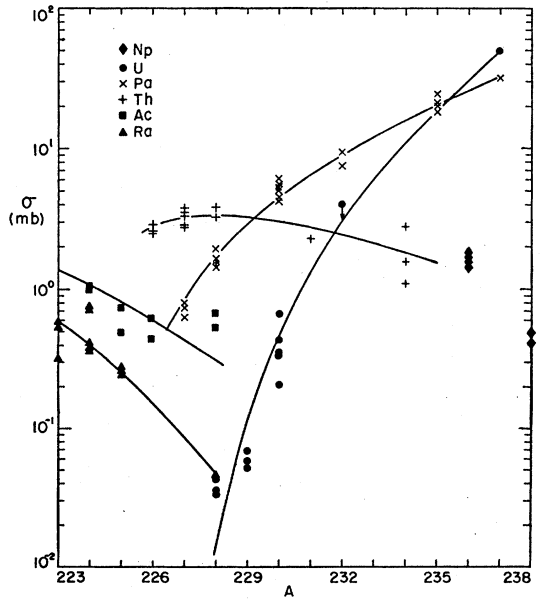

FIG. 1. Formation cross sections of disintegration products of U^{238} bombarded with 340-Mev protons.

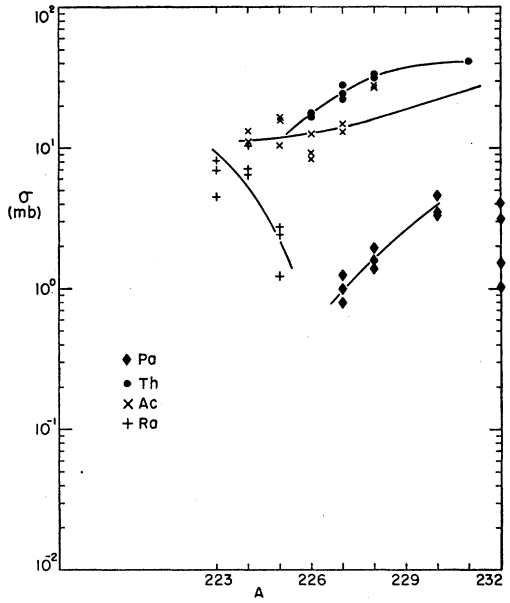

FIG. 2. Formation cross sections of disintegration products of Th^{232} bombarded with 340-Mev protons.

at these energies, formation is by knock-on reactions, the ratio of the yields for the (p,pn) and $(p,2p)$ reactions being very approximately that in which neutrons and protons occur in the nucleus. Caretto and Friedlander[20] showed this to be true for Ce^{142} irradiated with 380-Mev protons.

Spallation and Cross Sections

From the smooth curves of Figs. 1 and 2, the cross sections for a given mass number were calculated by summation of the cross sections for individual nuclide formation. Graphical summation of these values should then yield the spallation cross sections for uranium and

[20] A. A. Caretto and G. Friedlander, Phys. Rev. 99, 1649 (A) (1955).

thorium. For both cases, alpha-particle instability precluded cross-section measurements below mass number 223. Thus, for thorium, data were obtained for only nine mass numbers, but for uranium, it was possible to obtain data for fifteen mass numbers. Inspection of Fig. 3 indicates that the measured values represent essentially the entire cross section in the case of uranium, but that for thorium, an unknown—and possibly large—fraction could not be measured below mass 223. An attempt was made to infer yields of a few such nuclides through cross-section measurements of Po^{210}, At^{210}, and Bi^{210} formation. Although these nuclides could conceivably arise by direct formation, it is more likely that they would result from a series of short-lived alpha-particle emitters whose origin would be nuclides formed directly in spallation. For example, in uranium spallation, Po^{210} might arise from U^{226} or

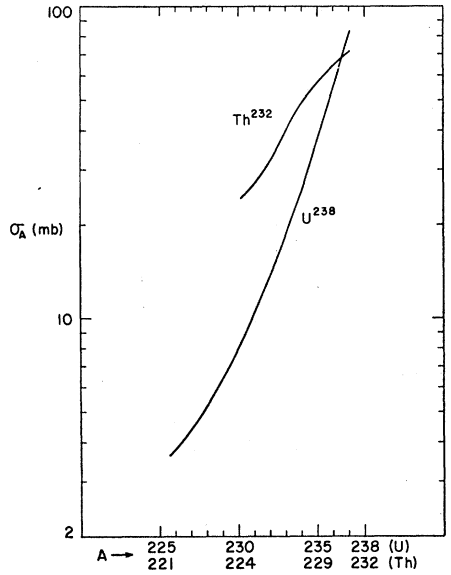

FIG. 3. Mass-number dependence of formation cross section of spallation products of U^{238} and Th^{232} irradiated with 340-Mev protons.

Th^{222}, while Bi^{210} would arise from Pa^{226} or Ac^{222}; in thorium spallation the directly-formed percursors would include Th^{222}, Ra^{218}, and Ac^{222}, Fr^{218}, respectively. In principle then, the curves in Figs. 1 and 2 could be used to decide which precursor(s) would be most consistent with the experimental data for the Po^{210}, Bi^{210}, and At^{210} cross sections.

Experimentally, Po^{210} was measured at times immediately after, one day after, and several weeks after, irradiation in order to measure the contributions from Po^{210}, At^{210}, and Bi^{210}, respectively. Unfortunately the data shown in Table III proved to be subject to such large errors (in some cases almost an order of magnitude) that they can be considered as semiquantative only.

Although the data proved to be too rough to infer the cross sections accurately for the very neutron-deficient spallation products, the relative magnitudes for thorium and uranium targets are certainly consistent with predicted cross sections for the probable precursors.

TABLE III. Cross sections, in millibarns, for formation of nuclides in the region of polonium.

Target	Product	340 Mev	300 Mev	250	200	100
U^{238}	At^{210}	1.2	...	...	0.08	...
	Po^{210}	1.7	...	...	0.17	...
	Bi^{210}	1.6	...	...	1.1	...
Th^{232}	At^{210}	2.4	15	13	11	0.3
	Po^{210}	13	7.8	4.7	...	~0
	Bi^{210}	26	8.1	14	11	1.1

Recently, Hutchin[21] has accurately measured the excitation function for Bi^{210} formation from U^{238} and Th^{232} bombarded with high-energy protons and has shown that the magnitudes of the cross sections given in Table III are correct. His excitation function for Bi^{210} from thorium closely resembled those for Ac^{225} and Ac^{226} obtained from thorium by Hyde,[22] indicating that Ac^{222} was probably the principal (though not the sole) precursor; of two other possible precursors Pa^{226} and Fr^{218}, the former would be predicted from Fig. 2 to make a relatively small contribution, and the latter was not measurable because of half-life considerations and lack of a suitable carrier or tracer. For U^{238} bombardment, Hutchin's data suggest that the main source of Bi^{210} was Ac^{222}.

The polonium data do demonstrate that neutron-deficient spallation products are formed with considerably higher cross section from thorium than from uranium. Thus, the spallation cross section can be measured essentially in its entirety for U^{238}, but for Th^{232} the value must be higher than the value obtained from Fig. 3. Graphical summation in Fig. 3 yielded 280 millibarns for U^{238}, and a minimum value of 370 millibarns for Th^{232}.

This and related information are summarized in Table IV.

The sum of the fission and spallation cross sections for U^{238} indicates agreement with the measured inelastic cross section. This is reasonable in view of the apparent completeness of the spallation cross section obtained from Fig. 3. However, if the same inelastic collision cross section is assumed for both Th^{232} and U^{238}, it is

TABLE IV. Inelastic cross sections (in barns) of U^{238} and Th^{232} for 340-Mev protons.

Target nucleus	σ_{fiss}[a]	σ_{spall}	$\sigma_{fiss}+\sigma_{spall}$	σ_{inel}[b]	% spall
U^{238}	1.37	0.28	1.65	~1.6	15
Th^{232}	0.80	>0.37	>1.2	...	>30

[a] See reference 15.
[b] See table, p. 1273, reference 14.

[21] W. H. Hutchin (unpublished data).
[22] E. K. Hyde and S. Skirvin (unpublished data).

evident that approximately 0.4 barn—or about 50%—of the spallation cross section for Th^{232} was not measured. Presumably this contribution to the cross section is to be found in the neutron-deficient isotopes of thorium, actinium, radium, and francium, a small fraction of which is evident from the polonium data in Table III.

Competition between Fission and Nucleon Evaporation

Serber[12] has adequately described the process for high-energy nuclear reactions at energies not complicated by meson production. According to this theory, an incident high-energy nucleon interacts with the nucleus through collisions with target nucleons, generating a nucleonic cascade in times of the order of the nuclear period for the high-energy nucleons. The cascade nucleons will either have left the nucleus in times of this order of magnitude or will have been captured and have distributed their energy to the remaining nucleons in such a manner that the nucleus will have come into a temperature equilibrium.

Using experimental *n-n* and *n-p* scattering cross-section data together with restrictions imposed by the Pauli principle, Goldberger[23] treated the cascade phenomenon for lead nuclei by Monte Carlo methods and was able to obtain satisfactory agreement with some experimentally observed quantities. The method has since been used by Bernardini, Booth, and Lindenbaum[24] and by McManus, Sharp, and Gellman[25] to carry out more extensive calculations. The latter investigators[26] have calculated the energy distribution to be expected for the residual nuclei following the cascade phase resulting from (among others) 400-Mev incident protons on U^{238} nuclei. Since their data indicate that an average of 1.6 cascade neutrons and 1.3 cascade protons (including the incident proton) are ejected in this phase, it is reasonable to assume that formation of an excited U^{236} or U^{237} nucleus should be a relatively probable event.

In the second phase of the nuclear reaction, nucleon evaporation occurs in times long compared with the times required for the first phase. It is presumably during this second phase that fission becomes a competing process. It has been shown by Heckrotte[27] that for U^{238} nuclei excited to about 100 Mev, evaporation of protons can be neglected as compared with that of neutrons. He has calculated the relative probabilities for emission of a given number of neutrons from uranium nuclei excited to 50 Mev and to 100 Mev.

Since, in a cascade process for 340-Mev protons, the average number of *additional* cascade nucleons ejected may be taken to be between one and two neutrons,[25] a heavy uranium nucleus, such as U^{236} or U^{237} may, to a first approximation, be taken as the most probable product of the cascade process. From the calculations of McManus *et al.*,[25] the distribution of nuclear excitation energies resulting from 400-Mev protons incident upon U^{238} nuclei was coupled with Heckrotte's treatment[27] to arrive at a final distribution of uranium nuclei after neutron evaporation. The crudeness of this calculation must be emphasized since it has been assumed that only heavy uranium nuclei exhibit McManus' nuclear excitation distribution. Nevertheless, such crude calculations imply that the yield of uranium isotopes over ten mass numbers would not vary by more than a factor of two or three. Comparison with the yield curve in Fig. 1 for uranium isotopes shows, however, that the the yields decrease by a factor of more than a thousand. Even if the above assumptions were to lead to conclusions in error by an order of magnitude, it is obvious from the low uranium yields that either proton emission cannot be neglected or that there is considerable competition from fission. The answer may be found in comparison of this curve with the analogous case in Fig. 2 for thorium isotopes. This curve exhibits far less slope than the uranium curve in Fig. 1, and in fact gives fair qualitative agreement with the rough calculation above for uranium nuclei. Since fissionability appears to be a sensitive function of the Bohr-Wheeler parameter Z^2/A, it is reasonable that the comparatively low yields, especially for light uranium isotopes, are due to greater fission competition. On the other hand, one would not expect the charged-particle barrier restrictions to charge markedly for such a relatively small increase in atomic number. It seems likely therefore, that fission, rather than proton emission, is responsible for the slope characteristic of the analogous yield curves in Figs. 1 and 2. It is probably significant that the slopes of the mass-yield curves decrease with the nuclear charge of the product nucleus; this might be expected from the fact that the fissionability parameter of Pa isotopes is less than that of uranium isotopes of the same mass number. The negative slopes for the radium and actinium yield curves of Fig. 1 reflect both the negligible extent of fission competition and the improbability of a high ratio of proton-to-neutron loss by the combined knock-on and evaporation phases.

Large yields of uranium and protactinium nuclides close to the target nucleus are, of course, characteristic of the nucleon-nucleon character of high-energy reactions. Analogous yields have been observed in all radiochemical studies.[1–10]

From the data of Fig. 1, Batzel[28] has attempted to evaluate the competition between neutron evaporation

[23] M. L. Goldberger, Phys. Rev. **74**, 1269 (1948).
[24] Bernardini, Booth, and Lindenbaum, Phys. Rev. **88**, 1017 (1952).
[25] McManus, Sharp, and Gellman, Phys. Rev. **93**, 924 (A) (1954).
[26] H. McManus *et al.* (private communication).
[27] W. Heckrotte, U. S. Atomic Energy Commission Report TID-2014 (unpublished).
[28] R. E. Batzel, University of California Radiation Laboratory Report UCRL-4303 (unpublished).

and fission, and has concluded that attainment of the critical nuclear distortion competes with neutron emission in a manner independent of the particular nuclear excitation, even though the actual process of division into two fission fragments might not occur until the nucleus has reached the final stages of cooling by nuclear evaporation. Conversely, the assumption that fission did not compete until the final stages in the evaporation process did not seem to fit the data as well; adjusted formation cross sections for individual product nuclides did not add up to the known inelastic cross section for uranium irradiated with protons in the region of 300 Mev.[14]

The relative importance of fission of lighter nuclei in uranium and thorium may be further shown from a comparison of the apparent loss of charged particles in nuclear reactions with 340-Mev protons. The cross sections for total neutron and total (apparent) proton production have been calculated in Table V; the last column gives the ratio of these quantities. For this calculation, the role of alpha-particle emission is ignored.

Since the lighter isotopes resulting from thorium spallation could not be measured, only a lower limit could be set on the numbers of neutrons and protons lost per nonfissioning collision in thorium. Of these two calculations, that for neutron loss will be the more underestimated. For this reason, the neutron-to-proton ratio in the last column is also a lower limit. The contrast between the σ_{1n}/σ_{1p} ratios for thorium and uranium can be attributable only to competition from the fission process among the neutron-deficient spallation products. The small value of this ratio for uranium simply reflects the greater extent of fission.

TABLE V. Neutron and proton loss in uranium and thorium irradiated with 340-Mev protons.

Target	$\sigma_{1n}/\sigma_{\text{spall}}$	$\sigma_{1p}/\sigma_{\text{spall}}$	σ_{1n}/σ_{1p}
U^{238}	3.0	1.75	1.7(5)
Th^{232}	>3.5	>1.4	>2.5

Comparison with Data from Photographic Emulsions

Ivanov, Perfilov, and Shamov[29] determined the prong distribution in uranium-impregnated *G*-5 emulsions accompanying forty-six fission events induced with 460-Mev protons. The number of prongs per event varied from zero to six, and included both knock-on and evaporation charged particles. Since the latter comprised only about 30% of the total charged particles, and of these only about 40% were alpha particles, to a first approximation each prong may be interpreted as a loss of one proton. Thus a one-prong star would result in a uranium nucleus, a two-prong star in a protactinium nucleus, etc. In the second column of Table VI the data of these investigators are listed as the frequency of a given prong distribution *vs* the atomic number of the resultant nucleus in the star accompanying the fission event. In the third column, the percent of the nonfissioning events occurring in each element is given for uranium spallation obtained by summation of the cross sections for the individual isotopes of each element in Fig. 1. Since even the most naive type of calculations, which attempted to adjust the observed spallation cross sections for fission competition, would lead to values for percent fissions which would greatly favor uranium (and possibly neptunium) isotopes, it would appear that a discrepancy with the film data in the second column of Table VI arises. The difference in the incident proton energies considered is not likely to be the cause of the discrepancy. This apparent disagreement may, however, be taken as an indication that although the probability for proton evaporation in an excited nucleus is very low, this probability will increase greatly once an excited nucleus has become "destined" to fission. Thus proton emission in the fragments—or partially formed fragments—may not be negligible, because of the considerably lowered barrier. In this manner, a low spallation cross section for formation of a low-mass uranium isotope might be interpreted as being due to fission competition. On the other hand, the same event might be detected in an emulsion as a two-prong (or greater) star.

TABLE VI. Distribution of fission events and nonfission events in uranium bombarded with high-energy protons.

Element	Percent of fissions 460-Mev protons[a]	Percent of nonfissions 340-Mev protons
Np	17±6	2
U	34±9	48
Pa	29±9	35
Th	17±6	13
Ac	4±3	2

[a] See reference 29.

Excitation Functions for Spallation Products of Uranium

The data of Table I giving the energy-dependence of a number of cross sections have been plotted in Fig. 4. Except for U^{237} all seem to have thresholds in the region of 50 to 100 Mev. Of these, the excitation functions for isotopes of uranium seem to show far less variation than the others, in the energy region from 100 to 340 Mev. In fact, mass-yield curves for uranium isotopes at different energies, similar to that in Fig. 1, seem to exhibit an energy invariance as compared with those for Th, Pa, Ac, etc. Since it is reasonable that a given distribution of uranium isotopes should be associated with a certain amount of fission, the invariance of the distribution implies that the same fission cross section

[29] Ivanov, Perfilov, and Shamov, Doklady Akad. Nauk SSSR **103**, No. 4, 573 (1955) (translated by Consultants Bureau, New York).

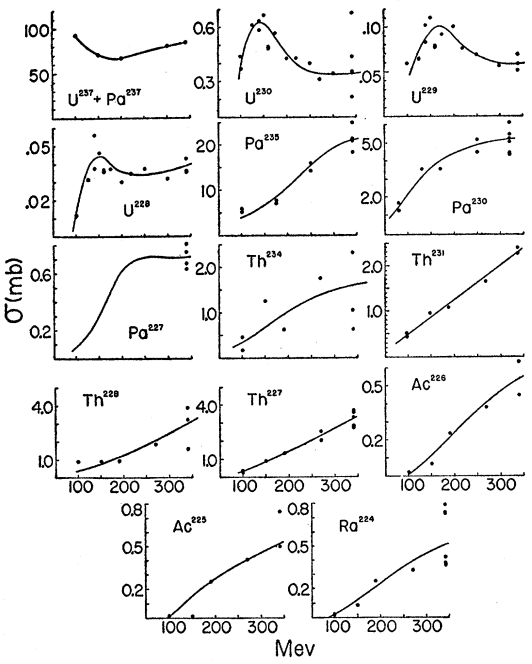

FIG. 4. Energy dependence of formation cross sections of spallation products of U^{238} bombarded with high-energy protons.

is due to uranium isotopes from 100 Mev to 340 Mev. Now Jungerman and Steiner[15] have shown that the fission cross section for proton-bombarded uranium is constant from 100 Mev to 340 Mev. It would therefore appear that the fraction of the fissions occurring in uranium which are actually due to uranium nuclei is also reasonably constant over this energy region. However, the distribution over all fissioning atomic numbers must certainly vary over this energy interval; at 50 to 100 Mev the fission contributions from Pa, Th, Ac, etc., decrease to zero. On the other hand, that from neptunium isotopes must become increasingly important at low energies owing to the increase in (p,xn) cross sections at decreasing energies. In fact, the data of McCormick and Cohen[30] show that the flat portion of the fission excitation function extends down to about 22 Mev, and at these energies neptunium isotopes may even become the principal fissioning type of nucleus.

APPENDIX. CHEMICAL SEPARATIONS

Protactinium.—Protactinium was obtained in a state of sufficient purity through extraction into diisopropylketone, first from a hydrochloric acid solution, then by a similar extraction from a nitric acid medium.

Thorium and Actinium.—The thorium and actinium were carried in a preliminary step on lanthanum fluoride in order that these be separated from all elements but the rare earths and other actinide elements.

The thorium was separated from actinium and the rare earths by extraction from a solution at a pH of 1.5 into a benzene solution of thenoyltrifluoroacetone. Actinium and the rare earths were then extracted into the same reagent at a pH of 5.7. Since no isotope of actinium exists with the desirable properties of a satisfactory tracer, no attempt was made to separate actinium from the carrier lanthanum and the rare earths, the lanthanum being used to determine chemical yield of the actinium on the assumption that the two were chemically indistinguishable through the procedure adopted.

Neptunium.—Neptunium was isolated through two extraction cycles from dilute hydrochloric acid into a benzene solution of thenoyltrifluoroacetone. Protactinium contaminant was removed by extractions from an acid solution into diisopropylketone.

Uranium.—The separation scheme for uranium involved an extraction into diethyl ether from a concentrated solution of magnesium nitrate, followed by adsorption, from concentrated hydrochloric acid, onto an anion exchange resin and elution with dilute acid.

Radium.—Barium was used as a carrier for radium, and purification therefore consisted of the usual methods employed for barium. Since the long-lived isotope Ra^{226} proved, in this work, to be somewhat unsatisfactory as a tracer isotope (because of a series of short-lived daughters), no attempt was made to separate barium and radium. Rather, barium was used to determine the chemical yield for radium on the assumption that they were chemically indistinguishable. Specific activities were, fortunately, high enough that the essentially

TABLE VII. Methods applied to nuclide detection.

Nuclide	Method
Np^{238}	Pulse analysis, Pu^{238} daughter
Np^{236}	Pulse analysis, Pu^{236} daughter
U^{232}	Pulse analysis
U^{230}	Pulse analysis
U^{229}	Alpha decay
U^{228}	Alpha decay
Pa^{235}	Beta decay
Pa^{233}	Beta decay
Pa^{232}	Isolation and pulse analysis, U^{232} daughter
Pa^{230}	Pulse analysis, U^{230} series
Pa^{228}	Isolation and pulse analysis, Th^{228} daughter
Pa^{227}	Alpha decay
Th^{234}	Beta decay
Th^{231}	Beta decay
Th^{228}	Pulse analysis
Th^{227}	Pulse analysis
Th^{226}	Alpha decay
Ac^{228}	Isolation and pulse analysis, Th^{228} daughter
Ac^{226}	Alpha decay, Th^{226} daughter series
Ac^{225}	Alpha decay
Ac^{224}	Isolation and pulse analysis, Ra^{224} daughter series
Ra^{228}	Isolation and pulse analysis, Th^{228} daughter
Ra^{227}	Isolation and pulse analysis, Th^{227} daughter series
Ra^{225}	Isolation and pulse analysis, Ac^{225} daughter series
Ra^{224}	Alpha decay
Ra^{223}	Pulse analysis
Po^{210}	Pulse analysis and alpha decay

[30] G. H. McCormick and B. L. Cohen, Phys. Rev. **96**, 722 (1954).

weightless plates necessary for satisfactory pulse analyses could be easily achieved.

Polonium.—Polonium was chemically plated on a silver disk immersed in a dilute nitric acid solution of the uranium target.

Methods of Radiation Detection.—The methods used to determine quantitatively the presence of a particular isotope included beta-particle decay, alpha decay, alpha pulse-height distribution analysis, and parent-daughter separations. Table VII lists in some detail these methods as they apply to the specific nuclide.

ACKNOWLEDGMENTS

The authors wish to thank Mr. James T. Vale and the crew of the 184-inch Berkeley cyclotron for making the irradiations possible, Miss M. Gallagher for technical assistance, and Dr. Kenneth Street for originally suggesting the need for such a study.

PHYSICAL REVIEW VOLUME 103, NUMBER 2 JULY 15, 1956

Electron Double Scattering by Nuclear Magnetic Moments*

ROGER G. NEWTON
Department of Physics, Indiana University, Bloomington, Indiana
(Received March 30, 1956)

Polarization effects in the scattering of high-energy electrons by charges and magnetic moments are discussed. A double scattering experiment using targets with lined-up nuclear spins should be a sensitive means of obtaining information about a possible difference in the charge and magnetic moment distributions of nuclei.

I. INTRODUCTION

FOR some time now electron scattering by nuclei has served as a tool for the determination of the shape of the nuclear charge distribution.[1] So sensitive has this technique become that it has begun to yield information about the shape of the magnetic moment distribution as distinct from that of the charge. Although in the only case measured so far, the proton, no difference between the two distributions was detected,[2] one might, on the basis of the shell model, expect the two distributions to be significantly different for nuclei other than those of hydrogen.

The purpose of the present note is to exhibit the results one could expect from another scattering experiment more specifically suited to the direct measurement of the effects of the nuclear magnetic moment. Such an experiment would involve the detection of the polarizing effect of a scattering by nuclei whose magnetic moments point in a prescribed direction. Unfortunately, no feasible experimental techniques are at present available for lining up nuclear spins for such a purpose. Presumably, however, it is but a question of time (and perhaps not a very long one, at that) that they will be. In that event the experiment here proposed would become possible.

* Supported in part by the National Science Foundation.

[1] Particularly the experiments by the group at Stanford. See Hahn, Ravenhall, and Hofstadter, Phys. Rev. **101**, 1131 (1956), and previous papers mentioned there.

[2] R. Hofstadter and R. W. McAllister, Phys. Rev. **98**, 217 (1955); R. Hofstadter and E. E. Chambers, Bull. Am. Phys. Soc. Ser. II, **1**, 10 (1956).

II. GENERAL DISCUSSION

We can very easily get an idea of the relative order of magnitude of the magnetic moment effects in scattering. While the measure of the strength of the Coulomb interaction is eZ, e being the electronic charge and Z, the atomic number of the nucleus, the measure of the magnetic moment interaction is $|\mathbf{p}|\mu$, where $\mathbf{p}$ is the momentum of the scattered electron and μ, the magnetic moment of the nucleus. The relative size of the two effects will therefore be of the order of magnitude

$$\frac{|\mathbf{p}|\mu}{eZ}=\frac{1}{2}\frac{|\mathbf{p}|}{Mc}\cdot\frac{\mu/\mu_N}{Z},$$

where μ_N is the nuclear magneton, and M is the proton mass. The energies used now or shortly to be used in electron scattering, of the order of one Bev or higher, are therefore large enough to produce sizable magnetic effects. It is also clear then that the effects are biggest for small values of Z.

The specific effects of the magnetic moment interaction which cannot be produced by the Coulomb field, are due to its noncentral nature, i.e., the fact that it contains a preferred direction. They are therefore not obtainable from a target whose nuclear magnetic moments are oriented at random. Those results (antisymmetries, etc.) which are obtainable from unoriented scatterers are also, qualitatively, obtainable from a pure Coulomb field and are therefore much harder to disentangle from those of the latter alone. Since the aim is to pin down experimentally the specific magnetic moment phenomena, we will be primarily interested in